Magnetic Resonance in Medicine 65:305–312 (2011)

Longitudinal MR Assessment of Hypoxic Ischemic Injury in the Immature Rat Brain

Yohan van de Looij,[1,2*] Alexandra Chatagner,[1] Petra S. Hüppi,[1] Rolf Gruetter,[2–4] and Stéphane V. Sizonenko[1]

Extremely preterm infants commonly show brain injury with long-term structural and functional consequences. Three-day-old (P3) rat pups share some similarities in terms of cerebral development with the very preterm infant (born at 24–28 weeks of gestation). The aim of this study was to assess longitudinally the cerebral structural and metabolic changes resulting from a moderate neonatal hypoxic ischemic injury in the P3 rat pup using high-field (9.4 T) MRI and localized ^{1}H magnetic resonance spectroscopy techniques. The rats were scanned longitudinally at P3, P4, P11, and P25. Volumetric measurements showed that the percentage of cortical loss in the long term correlated with size of damage 6 h after hypoxia–ischemia, male pups being more affected than female. The neurochemical profiles revealed an acute decrease of most of metabolite concentrations and an increase in lactate 24 h after hypoxia–ischemia, followed by a recovery phase leading to minor metabolic changes at P25 in spite of an abnormal brain development. Further, the increase of lactate concentration at P4 correlated with the cortical loss at P25, giving insight into the early prediction of long-term cerebral alterations following a moderate hypoxia–ischemia insult that could be of interest in clinical practice. Magn Reson Med 65:305–312, 2011.

Key words: magnetic resonance spectroscopy; hypoxia–ischemia; immature pup rat brain; 3 days old

Brain injury in the very preterm infant (born at 24–28 weeks of gestation) remains an important health problem: of those infants with a birth weight under 1500 g, 25%–50% later exhibit developmental disabilities and up to 5%–15% having cerebral palsy (1). The pattern of brain injury associated with prematurity is unique with a specific loss of developing cerebral gray and white matters (2). The 3-day-old (P3) rat shares some similarities in terms of cortical neuronal, glial, and oligodendroglial development with the very preterm infant corresponding to a human preterm brain development at 24–28 weeks of gestation (3). Furthermore, cerebral injuries seen in the P3 rat pup following hypoxia–ischemia (HI) are related to those of early preterm infants with white matter injury and altered cortical development (4,5). Several previous studies have shown gender vulnerability differences following HI on the P7 rat pup brain related to different mechanisms of cellular death after neonatal brain injury in males and females (6–8) but a difference in this very early injury has been less studied.

Magnetic resonance imaging (MRI) techniques have been widely used to study normal or pathological rodent brain cerebral development (9–13). Several authors have performed conventional MRI techniques in the early stage following HI induced in P7 rat pup brain (10,12), but consequences of early HI in the very immature P3 rat pup brain are less frequently investigated (11). Sizonenko et al. (11) performed MR diffusion tensor imaging (DTI) after HI at P3, showing acute reduced apparent diffusion coefficient and fractional anisotropy in the ipsilateral cortex that persisted at P6. Cortical eigenvector maps derived from diffusion tensor images revealed microstructural disruption of the radial organization corresponding to regions of neuronal death, radial glial disruption, and astrocytosis. These microstructural modifications might induce permanent changes in the development of the brain, and only longitudinal studies will probe more accurately modifications of the developing brain architecture following HI (11). More recently, Yang et al. (13) have detected cortical gray matter lesion in the late phase of mild HI injury by manganese-enhanced MRI. Human MRI studies in preterm infants have not only shown white matter damage but also developmental alteration of gray matter (14,15).

Recently, with the development of advanced localized ^{1}H magnetic resonance spectroscopy (^{1}H MRS) technique at high magnetic field, it has been possible to follow the changes in "neurochemical profile" of the rat brain during cerebral development (16). This technique allows assessment of several metabolite concentrations (the neurochemical profile), including antioxidants, compounds related to energy metabolism, neurotransmission, membrane precursor, osmoregulation, myelinization, neuronal markers, glial markers, and neuroprotection. Previous studies have shown that ischemia on adult rat brain leads to specific changes in the neurochemical profile (17). In view of the ability to perform longitudinal

[1]Department of Pediatrics, Division of Child Development and Growth, University of Geneva, Geneva, Switzerland.

[2]Laboratory for Functional and Metabolic Imaging (LIFMET), Ecole Polytechnique Fédérale de Lausanne (EPFL), Lausanne, Switzerland.

[3]Department of Radiology, University of Lausanne, Lausanne, Switzerland.

[4]Department of Radiology, University of Geneva, Geneva, Switzerland.

Yohan van de Looij and Alexandra Chatagner contributed equally to this study.

Grant sponsor: Swiss National Fund; Grant number: 31003A-112233; Grant sponsors: ELA Foundation, NEOBRAIN (EC-6thFP), Centre d'Imagerie Biomédicale, Leenards and Jeantet Foundations.

*Correspondence to: Yohan van de Looij, Ph.D., Laboratory for functional and metabolic imaging, Ecole Polytechnique Fédérale de Lausanne, CH F1 602, Station 6, 1015 Lausanne, Switzerland. E-mail: yohan.vandelooij@epfl.ch

Received 12 February 2010; revised 29 July 2010; accepted 6 August 2010.

DOI 10.1002/mrm.22617
Published online 22 September 2010 in Wiley Online Library (wileyonlinelibrary.com).

studies and to translate observations made to humans, ^{1}H MRS was chosen to assess the acute and long-term metabolic effects of HI on the immature brain.

The aims of this study were to monitor volumetric and metabolic changes with time and to establish relationship with subsequent permanent changes in cerebral development, with a particular attention to gender differences, in a model of neonatal HI injury in the P3 rat pup brain using high-field MRI and ^{1}H MRS techniques.

MATERIALS AND METHODS

The Geneva School of Medicine Animal Ethics Committee and the Geneva State Veterinary Service approved these studies.

Animal Model

The unilateral HI model has been described previously (4,5). Briefly, 3-day old (P3) Wistar pups had right carotid cauterization under isoflurane anesthesia. After a 30-min recovery period at 37°C, they underwent 6% O_2 hypoxia for 30 min in the same thermoneutral conditions. The pups then were returned to the dam and maintained in normal holding conditions.

NMR Measurements

Five hours (P3), 24 h (P4), 8 (P11) days, and 22 (P25) days after HI, each rat pup was placed supine within an adapted rat holder to perform the MR scans. Throughout the MR experiment, they were continuously anesthetized under a flow of 1.5%–2% isoflurane in oxygen. The rat body temperature was maintained at 37°C using a thermoregulated water circulation system placed under the rat bed. Respiration and heart rate were also monitored during MR acquisition.

Animal Groups

Two groups were investigated: a HI group showing damage in the ipsilateral cortex, but not in the contralateral cortex, and a control group. The rats of the control group were not submitted to surgery and HI but underwent MRI scans under the same conditions as the HI group. The experiments were performed longitudinally using for the HI group: eight rats from P3 to P25, 10 rats from P3 to P11, and 13 rats from P3 to P4. For the control group, seven rats were scanned from P4 to P25.

MR Experiments

All MR experiments were performed on a 9.4-T/31-cm magnet (Magnex Scientific, Abington, UK) connected to Direct Drive console (Varian, Palo Alto, CA) equipped with 12-cm gradient coils (400 mT/m, 120 μsec). A homebuilt 17-mm-diameter ^{1}H quadrature surface coil was used for radiofrequency transmission and signal reception. Five hours following HI, T_2-weighted (T_2W) fast spin echo images with pulse repetition time/echo time = 4000/80 msec; field of view = 15 × 15 mm^2, a matrix size = 256 × 128, and eight averages were used to detect presence of injury. Following HI, at 1, 8, and 22 day(s) fast spin echo images were performed on each injured pup with the same parameters except the field of view = 20 × 20 mm^2 at P11 and P25. Twenty-five to 30 slices of 0.8-mm thickness were acquired depending on the size of the brain. Fast spin echo images were used to position the volume of interest (VOI) as well as to determine the brain volume and the lesion volume for each pup in the study.

For each time point, MRS VOI was carefully placed in the somatosensory cortex at the level of the ventral hippocampus (Fig. 3) corresponding to the site of the lesion in this model as reported previously (4,5,11,18). Depending on extent of cortical loss (CL) at P11 and P25, the VOI was positioned to avoid as much as possible partial volume effect from other brain structures such as hippocampus. However, some contaminations cannot be excluded. First- and second-order shims were adjusted for each VOI of 1.5 × 1.5 × 2.5 mm^3 using an echo-planar imaging version of the FASTMAP sequence (19). The water linewidth ranged from 8 to 12 Hz. First, a water spectrum was acquired as a reference for quantification (eight averages), then spectra from cortex were acquired using an ultrashort (echo time/pulse repetition time = 2.7/4000 msec) SPECIAL spectroscopy method. This method combines 1D image-selected in vivo spectroscopy in the vertical (Y) direction with a slice selective spin echo in the X and Z directions and provides full signal intensity available in the excited region (20). The spectra were acquired in 30 blocks of 16 averages saved separately for a total acquisition time of 32 min. Spectra were acquired in the lateral cortex at the level of the lesion (lesion, HI group), in the corresponding contralateral area in the HI group (contralateral, HI group), as well as in the corresponding cortical area on control pups (control, control group) at P4 (HI group: n = 13, control group: n = 7), P11 (HI group: n = 10, control group: n = 7), and P25 (HI group: n = 8, control group: n = 7). The number of rats scanned decreased over time (13, 10, and 8 rats at P4, P11, and P25, respectively): one rat died between P4 and P11 [a male with a percentage of injured cortex (%IC) equal to 43.6%] and two spectra were removed at P11 as well as two at P25 due to malfunctioning shim gradient, leading to increased linewidth and consequently insufficient signal-to-noise ratio (SNR). To assess longitudinally up to P25 the effects of HI in pup rat brain, all subjects scanned at P25 have also been scanned at P11 and P4.

Data Analysis

The 30 blocks were corrected for amplitude of static (polarizing) field shift before summation and then an eddy-current correction was applied. The metabolite concentrations were quantified using LCModel (21) that analyzed the spectrum as a linear combination of model spectra from individual metabolites according to previously described procedures (22). The water spectra were used as reference as in previous studies (16) assuming a water content of 88.0% in the rat brain at P4, 86.3% in the rat brain at P11, and 80.6% in the rat brain at P25 (16). To correct the water content in the lesion at P4, proton density images (a gradient echo multislices sequence, echo time/pulse repetition time = 3.6/2000 msec, flip angle = 45°) were performed on four injured

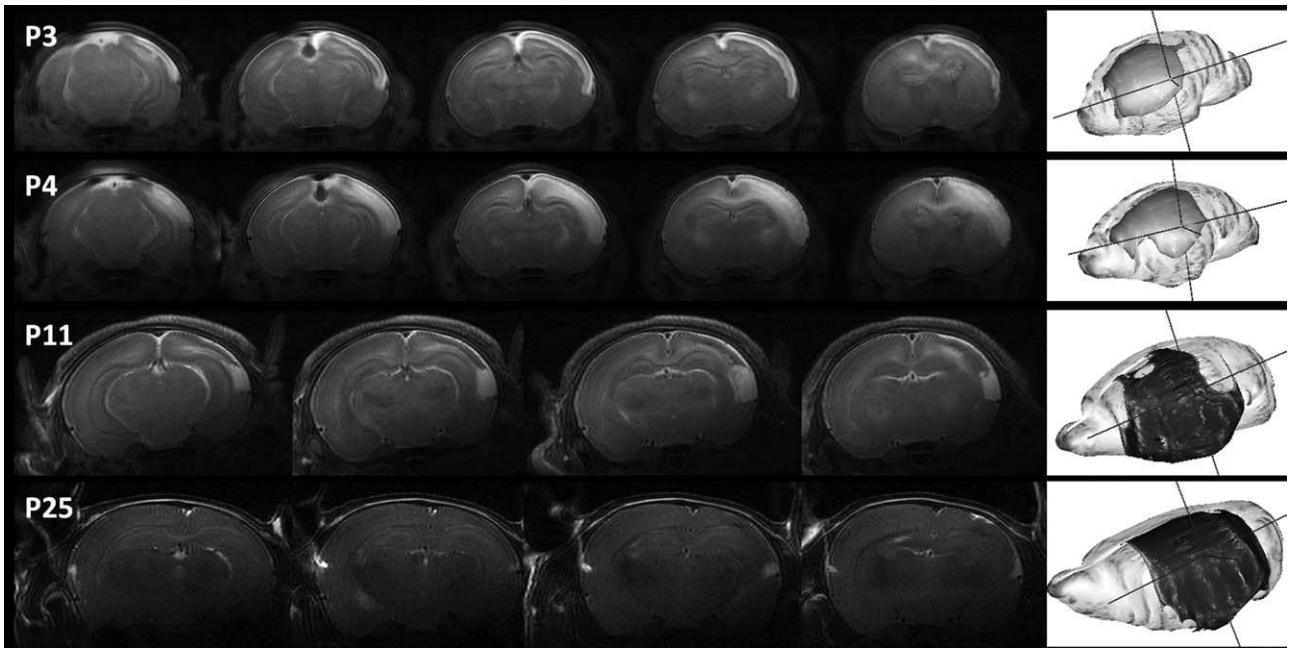

FIG. 1. T_2W images of a typical injured male rat pup at different time points [5 h (P3); 24 h (P4), 8 (P11) and 22 days (P25) after HI injury] showing the evolution of the ischemic lesion in the ipsilateral cortex. During the first 24 h, oedema develops gradually. P11 ipsilateral cortex shows a mix between lesion and beginning of CL. At P25, images present a large CL in the ipsilateral cortex. In the last column of each row, 3D reconstruction of the brain volume (transparent) and of the lesion (gray) at P3 and P4 as well as 3D reconstruction of the brain volume (transparent) and of the CL (black) at P11 and P25.

rat pups. An increase in average water content of 5% was observed in the lesion. As a result, a water content of 93.0% in the P4 injured rat brain cortex was assumed and used for metabolic concentration quantification.

The results provided the quantification of the following 17 metabolite concentrations: macromolecules (Mac), ascorbate (Asc), beta-hydroxybutyrate (bhB), phosphorylcholine (PCho), creatine (Cr), phosphocreatine (PCr), γ-aminobutyric acid (GABA), glucose (Glc), glutamate (Glu), glutamine (Gln), myo-inositol (myo-Ins), lactate (Lac), *N*-acetylaspartate (NAA), *N*-acetylaspartylglutamate (NAAG), phosphoethanolamine (PE), and taurine (Tau). The accuracy in the quantification is given by the Cramer-Rao lower bounds directly calculated by LCModel. The percentage of variation of metabolite concentration between ipsilateral and contralateral cortex at P4 was calculated to assess correlations with the percentage of cortical loss (%CL) at P25.

Volumetric measurements were manually performed using Anatomist/Brain Visa free software (23). At P3 and P4, ipsilateral cortical volume as well as lesion volume were measured to assess the %IC [%IC = (lesion volume/ipsilateral cortical volume) × 100]. At P11 and P25, measurements of ipsilateral cortical volume and contralateral cortical volume were performed to quantify the %CL {%CL = ([contralateral cortical volume − ipsilateral cortical volume]/contralateral cortical volume) × 100} following HI. Note that at P3–P4, the %IC was quantified on the hyperintense signal seen on T_2W images, and compared with the entire ipsilateral cortical volume whereas at P11–P25, the %CL was based on the difference between anatomical volumes of contralateral and ipsilateral cortices.

Statistical Analysis

A Mann Whitney test was used to compare concentrations measured within the damaged area of the HI group and in the same region in the control group as well as metabolite concentrations between males and females in the injured and control groups, respectively. Significant gender and time differences of the brain volumes (%IC at P3/P4 and %CL at P11/P25) were similarly compared. For both tests, P value under 0.05 was considered significant. Correlation coefficients between percentage of variation of metabolite concentration at P4 and %CL at P25 was assessed with Matlab (Mathworks, Natick, MA); correlation was considered as significant when $P < 0.05$.

RESULTS

Volumetric Measurements

Figure 1 shows multislice typical longitudinal T_2W fast spin echo image of a P3, P4, P11, and P25 HI rat pup brain. Early after injury (5 h), an increase in signal intensity was present in the ipsilateral cortex and was still apparent 24-h post-HI injury. At P11, the ipsilateral hypersignal decreased and was apparent on all the males but only on 37% of the females. At that time point, CL was already visible with a clear dissymmetry between ipsilateral and contralateral cortices. At P25, there was no signal intensity change, but MR images showed CL in the ipsilateral parietal cortex. On volumetric measurements, differences between males and females were detected for all the time points (Fig. 2A,B). At P3 and P4, the %IC was lower in females compared with males (P3: $P = 0.02$ and P4: $P = 0.04$), with no significant difference between the volume of injury at P3 and at P4.

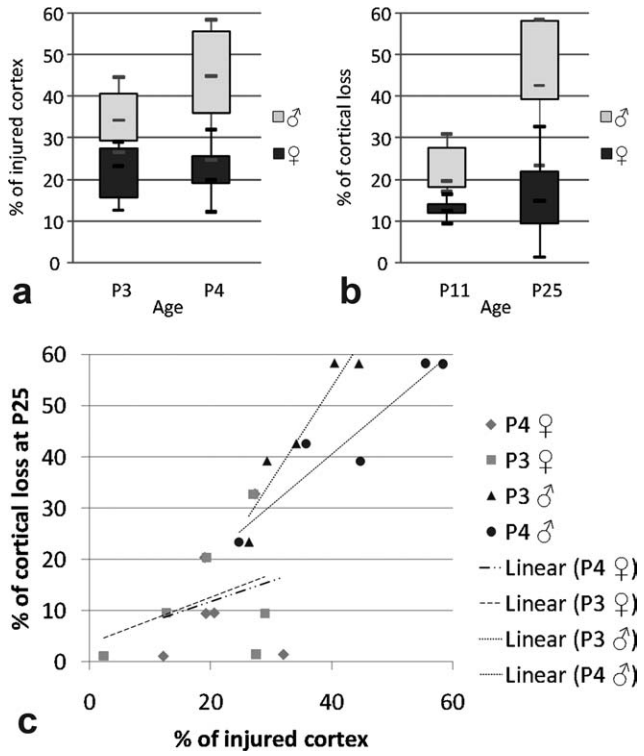

FIG. 2. **A**: Box plot of the %IC (calculated from the size of hyperintense signal on the T_2W images) as a function of age from P3 to P4 for the males and the females. **B**: Box plot of the %CL as a function of age from P11 to P25 for the males and the females. **C**: Scatter plots of the %CL at P25 as a function of the %IC at P3 and P4 for the males and the females. For all the figures, genders have been separated in regard to the differences in the lesion size.

Later, at P11 and P25, the %CL was found to be higher for the males compared with the females (P11: $P = 0.03$ and P25: $P = 0.02$), with an increased loss with time from P11 to P25 ($P = 0.02$). A strong correlation (Fig. 2C) between the %IC at P3/P4 and the %CL at P25 (P3: $r = 0.95$, $P = 0.013$; P4: $r = 0.94$, $P = 0.014$) was only found for the males, whereas for the females, no correlation was observed (P3: $r = 0.39$, $P = 0.45$; P4: $r = 0.23$, $P = 0.66$).

^{1}H MRS

In this study, FASTMAP shimming (first-order and second-order correction of the magnetic field homogeneity) enabled the realization of good-quality spectra. Because of very thin cortical structure in the rat pup brain, MRS was performed on a very small volume of 12 μL placed on the parietal cortex (Fig. 3). The average signal-to-noise ratio calculated on all acquired spectra (i.e., P4, P11, and P25) was 13 ± 4.

Such consistent data were subjected to spectral analysis and to absolute quantification by LCModel, thus providing the concentration of 17 metabolites ("the neurochemical profile"—Table 1). The Cramer-Rao lower bounds were below 20% for most of the metabolites in all age groups.

For all time points, there were no significant differences in metabolite concentrations measured in the IC of the males compared with the IC of the females ($P > 0.05$, data not shown). Indeed, no significant changes were found between males and females in the control group ($P > 0.05$, data not shown). As a result, males and females were pooled for MRS results to increase the statistical power.

At P4, the neurochemical profile of the lesion cortex indicated significant differences for several metabolites compared with the control cortex (Table 1). As summarized in Table 1, 24 h after HI injury and during the acute phase, concentrations of most of the quantified metabolites in the cortical lesion, such as [Mac], [Asc], [PCho], [Cr], [PCr], [GABA], [Glu], [myo-Ins], [NAA], [NAAG], [PE], [Tau], [NAA] + [NAAG](=[tNAA]), [Glu] + [Gln], [GPC] + [PCho](=[tCho]), and [Cr] + [PCr] (=[tCr]), as well as the ratio [Glu]/[Gln], were decreased. At the same time point, only [Lac] was found to be increased in the injured tissue.

At a later time point (P11), many of the differences disappeared with metabolites in the lesion cortex returning to similar level as in the control cortex. Noticeable significant changes were an increase of [Glc] and [Gln] resulting in a decrease of the [Glu]/[Gln] ratio. Furthermore, NAA and total NAA concentrations were found lower in the lesion cortex compared with control one.

For the last time point (P25), major part of the metabolite concentrations of the lesion cortex recovered showing no statistically significant difference compared with the control ones. The only decreases observed were [tNAA], [Glu] + [Gln], and [tCr].

The %CL at P25 was correlated with the percentage of increase of lactate concentration in the ipsilateral cortex at P4 (Fig. 4; $r = 0.57$, $P = 0.04$). No correlation between loss of cortex and other metabolite variations such as tNAA, tCr, or Glu + Gln was found significant (data not shown).

DISCUSSION

Volumetric Measurements

At P3 and P4, the injury was clearly visible as a hyperintense signal on the T_2W images due to presence of oedema 6 h following HI and persistent at 24 h postlesion. T_2W MRI has been widely used to detect presence and assess temporal evolution of cerebral oedema in animal model of ischemia (24,25) as well as in clinical practice (26). There were no significant differences in the %IC between P3 and P4 but, at both time points, cortex of male was more injured than that of female. Interestingly, a trend toward an increase in the volume of injury between these early time points was seen in males, reflecting persistent oedema expansion that was not present in the female brains (Fig. 2A). At P11, a remaining lesion (i.e., T_2W hypersignal) was apparent on all males but in only 37% of the females. Nevertheless, at this later time point, CL was higher for the males than for the females. Finally, at P25, CL was obvious and once again the %CL was higher for the males than for the females. HI led to a subsequent abnormal development of the brain with a major CL 22 days postinjury.

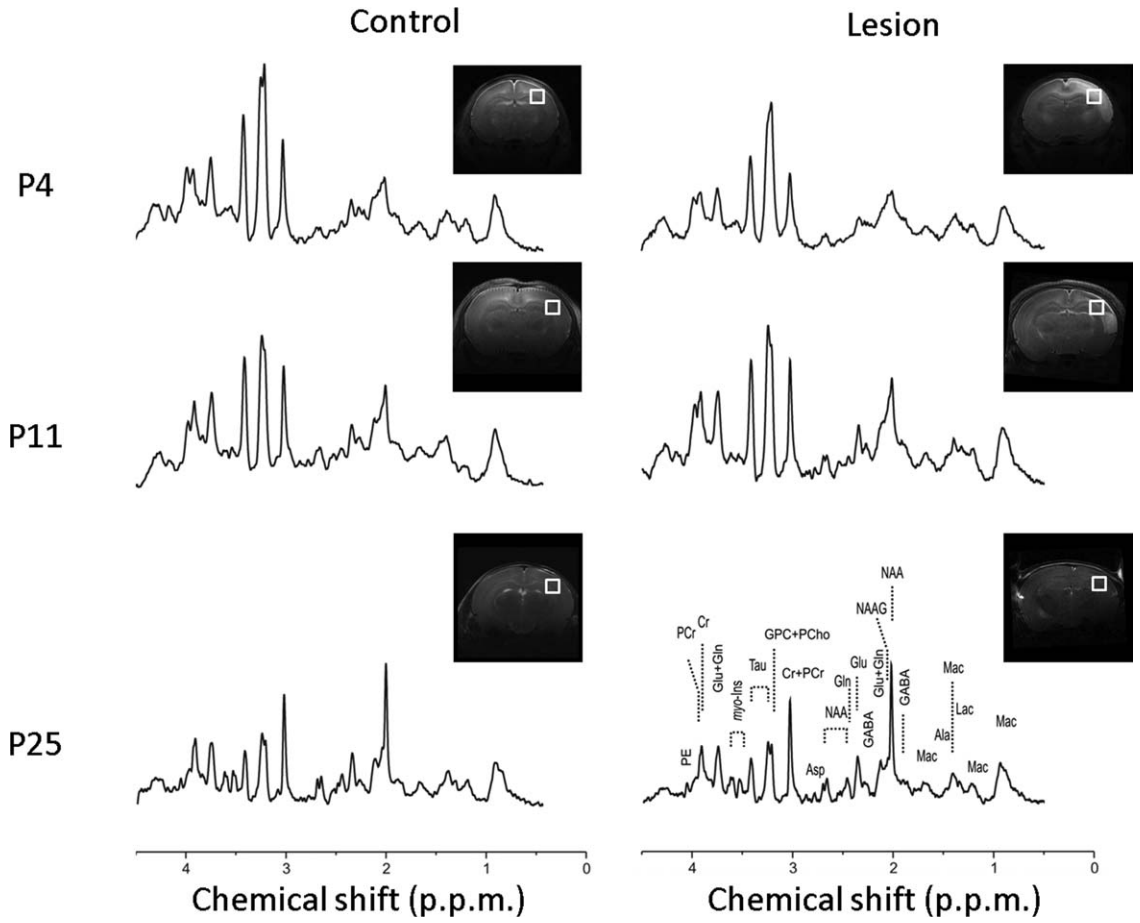

FIG. 3. Time course of in vivo localized ^{1}H NMR spectra in the cortex of a typical injured and a typical control rat pup from P4 to P25. Respective metabolite assignments are indicated on the P25 control spectrum. All spectra (SPECIAL, echo time/pulse repetition time = 2.8/4000 msec, number of transients = 320) were displayed with gaussian apodization (Gaussian filter = 0.1 sec). Abbreviations: Mac, macromolecules; Asc, ascorbate; bhB, beta-hydroxybutyrate; PCho, phosphorylcholine; Cr, creatine; PCr, phosphocreatine; GABA, γ-aminobutyric acid; Glc, glucose; Glu, glutamate; Gln, glutamine, myo-Ins, myo-inositol; Lac, lactate; NAA, *N*-acetylaspartate; NAAG, *N*-acetylaspartylglutamate; PE, phosphoethanolamine, and Tau, taurine.

The males were more damaged than the females at P3 and consequently had a major CL at P25. Indeed, only for the males, the percentage of cortex injured at P3/P4 correlated to the %CL at P25 (Fig. 2C). In our study, after the same HI injury, the damage in males appears more pronounced than in females leading to increased cerebral developmental abnormalities in males. The females that are less injured at the early stage are showing better recovery with a reduced CL compared with the males. This is consistent with the persistent hypersignal on T_2W images at P11 for all the males but for only 37% of the females. Even if the reason of these gender vulnerability differences is not fully known, it has been shown that mechanisms of cellular death after neonatal brain injury are not similar in males and females. In the immature male brains, neurons displayed a more pronounced translocation of apoptosis-inducing factor with mitochondrial outer-membrane permeabilization and cytochrome *C* release in the cytosol after HI. This major mitochondrial dysfunction in males is associated with an increased vulnerability to oxidative stress leading to increased production of oxidative species into the mitochondria. In the female brain, cell death is mediated by activation of plasma membrane death receptors and activation of the caspase cascade (6–8). It must be noted that the amount of CL remains similar between P11 and P25 in the females, whereas it increases in the males (Fig. 2B). The initial severity of damage could explain this gender-related evolution, but different mechanisms of repair and plasticity between males and females might also be involved (27). As a result, we conclude that early after HI injury (5 h), a gender difference in the response to the injury is already present, and the size of the lesion at P3 determines the level of cortical disruption for the males only.

^{1}H MRS

In the early phase (24 h), HI injury leads to major changes in the neurochemical profile in the IC compared with the control one. Most metabolites showed decreased concentrations except for Lac, which was increased, and bhB, Glc, and Gln that did not change significantly. The significant decrease of Mac—a putative tissue integrity marker—and of total Cho and PE, major components of cell membrane, provides in vivo evidence

Table 1
Neurochemical Profiles in Control Cortex (Ctl) and in the Lesion (Les) of Rat Pup at Different Time Points Following HI: P4, P11, and P25

Metabolites	P4 Ctl	P4 Les	P4	P11 Ctl	P11 Les	P11	P25 Ctl	P25 Les	P25
Mac	1.4 ± 0.1	1.1 ± 0.2	↓**	1.6 ± 0.2	1.5 ± 0.2		1.9 ± 0.2	1.9 ± 0.2	
Asc	4.3 ± 0.3	2.3 ± 0.9	↓**	3.7 ± 0.3	3.5 ± 0.6		3.8 ± 1.6	2.8 ± 0.7	
bHB	0.9 ± 0.3	1.2 ± 0.6		1.0 ± 0.6	1.0 ± 0.6		2.4 ± 2.0	0.4 ± 0.1	
PCho	1.8 ± 0.1	0.9 ± 0.2	↓***	0.9 ± 0.1	0.7 ± 0.1		0.6 ± 0.2	0.5 ± 0.2	
Cr	2.2 ± 0.3	1.6 ± 0.4	↓**	2.6 ± 0.3	2.3 ± 0.4		3.6 ± 0.5	3.3 ± 0.5	
PCr	3.6 ± 0.5	2.3 ± 0.7	↓***	4.5 ± 0.9	4.9 ± 0.7		4.2 ± 0.5	3.6 ± 0.6	↓*
GABA	1.5 ± 0.1	0.8 ± 0.2	↓***	1.6 ± 0.3	1.5 ± 0.2		1.8 ± 0.9	1.1 ± 0.5	
Glc	1.3 ± 0.3	2.3 ± 1.1		1.6 ± 0.4	2.3 ± 0.5	↑*	3.7 ± 1.6	2.8 ± 1.3	
Gln	1.4 ± 0.1	1.4 ± 0.5		1.4 ± 0.2	1.9 ± 0.5	↑**	3.3 ± 1.0	2.5 ± 0.7	
Glu	4.0 ± 0.3	2.4 ± 0.5	↓***	5.0 ± 0.6	4.9 ± 0.5		9.3 ± 1.3	7.3 ± 0.8	↓*
Ins	2.0 ± 0.3	1.2 ± 0.4	↓***	1.9 ± 0.3	2.2 ± 0.3		3.5 ± 1.4	4.0 ± 0.6	
Lac	1.0 ± 0.3	2.1 ± 1.1	↑*	1.6 ± 0.5	1.9 ± 1.4		1.3 ± 0.1	0.7 ± 0.2	
NAA	2.2 ± 0.1	1.5 ± 0.2	↓***	4.4 ± 0.5	3.7 ± 0.4	↓*	9.0 ± 0.8	7.5 ± 0.6	↓*
NAAG	1.3 ± 0.3	0.9 ± 0.2	↓**	1.0 ± 0.1	0.8 ± 0.3		0.9 ± 0.2	0.8 ± 0.4	
PE	6.5 ± 0.3	4.2 ± 1.1	↓**	6.1 ± 0.4	6.7 ± 1.0		3.5 ± 2.2	2.3 ± 0.5	
Tau	16.0 ± 0.9	8.9 ± 2.2	↓***	13.7 ± 0.3	12.5 ± 2.4		7.5 ± 0.6	8.3 ± 1.3	
NAA + NAAG	3.4 ± 0.3	2.4 ± 0.2	↓***	5.3 ± 0.6	4.4 ± 0.5	↓**	9.9 ± 1.0	8.2 ± 0.7	↓*
Glu + Gln	5.4 ± 0.3	3.8 ± 0.8	↓**	6.2 ± 0.9	6.9 ± 0.7		12.6 ± 1.8	9.8 ± 1.3	↓*
GPC + PCho	1.8 ± 0.1	1.1 ± 0.4	↓**	0.8 ± 0.1	0.7 ± 0.2		0.5 ± 0.3	0.6 ± 0.1	
Cr + PCr	5.8 ± 0.3	3.7 ± 0.8	↓***	6.8 ± 0.2	7.0 ± 0.8		7.9 ± 0.8	6.9 ± 0.5	↓*
PCr/Cr	1.7 ± 0.5	1.7 ± 0.6		1.7 ± 0.3	2.2 ± 0.6		1.2 ± 0.2	1.2 ± 0.3	
Glu/Gln	3.0 ± 0.5	2.1 ± 1.2	↓*	3.9 ± 1.0	2.6 ± 0.6	↓**	3.0 ± 0.9	3.2 ± 1.1	

All concentrations are presented as mean ± SD in mM/g except the ratios. For each time point, changes are displayed with specific orientated arrows: "↑", increase and "↓", decrease. The number of "*" represents significant level of $P < 0.05$, 0.01, and 0.001.
Abbreviations: Mac, macromolecules; Asc, ascorbate; bhB, beta-hydroxybutyrate; PCho, phosphorylcholine; Cr, creatine; PCr, phosphocreatine; GABA, γ-aminobutyric acid; Glc, glucose; Glu, glutamate; Gln, glutamine, myo-Ins, myo-inositol; Lac, lactate; NAA, *N*-acetylaspartate; NAAG, *N*-acetylaspartylglutamate; PE, phosphoethanolamine, and Tau, taurine.

of tissue and cells integrity disruption. The decrease of NAA, NAAG, and total NAA assumed to be neuronal markers further demonstrates the presence of neuronal damage. Both neuronal death and suffering can be reflected in these changes as NAA has been hypothesized as not only reflecting the number of neurons but also the functional status of the neurons (17). An acute neuronal disruption in this model has been clearly established previously using complementary methods of histology and DTI (4,11). Cell energy metabolism seemed to be conserved as depicted by the conservation of the [PCr]/[Cr] ratio.

The ischemic status of the brain is confirmed by the persistent increase of Lac 24 h after HI, providing evidence of anaerobic metabolism post-HI as previously described in several ischemic rat studies (28,29). The high levels of lactate found at 24 h might reflect production of lactate by phagocytic cells infiltrating the brain (28) or more likely relate to secondary energy failure that occurs after perinatal cerebral HI and mitochondrial dysfunction as reported by others (30,31).

Asc was also decreased, and this might be due to an increased consumption of Asc because of increased O_2 free radicals arising from the reperfusion/reoxygenation phase. In addition, the neurotransmission system was altered as suggested by the decrease of GABA—an inhibitory neurotransmitter, Glu—an excitatory neurotransmitter, and Tau, also implicated in neurotransmission. The decrease of Tau, which plays an important role in osmoregulation, could also be related to post-HI ionic pumps disturbance, leading to persistent cellular oedema 24 h postinjury. From the glutamate decrease, the ratio [Glu]/[Gln] was also decreased. The [Glu]/[Gln] ratio in normal brain is an important parameter, because Glu and Gln metabolism in the brain is closely related to neurotransmission and Glu and Gln cycling between neurons and glia (32). In addition, the decrease in [Glu]/[Gln] ratio from a normal value is known to be a marker of a dysfunction of the Glu–Gln cycle (33). To summarize: at P4, the modification of these metabolites reflects functional alterations of the IC in the acute phase post-HI injury.

At the second time point P11, most of the metabolites of the lesion cortex have recovered to a concentration close to the one measured in the control cortex except for NAA, total NAA, and Glu/Gln, which remain

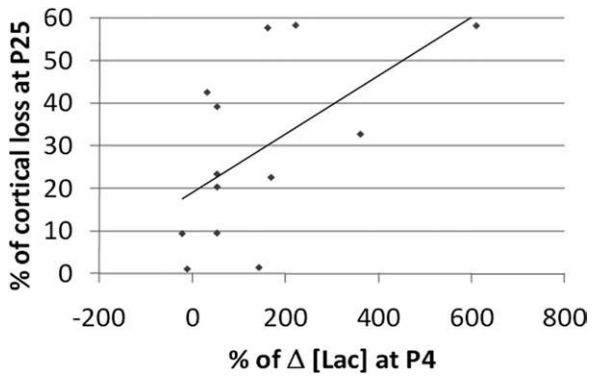

FIG. 4. Scatter plot of the %CL at P25 function of the percentage of variation of lactate concentration at P4 ($r = 0.57$, $P = 0.04$).

decreased, and Glc and Gln that are increased. The increase of Glc, which is known to be an energy source in the brain, could reflect increased energetic demand that would be probably related to an enhancement of intrinsic repair mechanisms taking place in response to tissue damage (34). Nevertheless, it is difficult to conclude as blood glucose has not been measured and several parameters can impact brain glucose concentration such as time after feeding or period of the day. The NAA and total NAA remain decreased confirming persistent neuronal injuries. The high concentration of Gln resulting in a decreased [Glu]/[Gln] provided evidence for persistent Glu–Gln cycle dysfunction probably related to astrogliotic reaction already shown in this model (11). For this second postinjury phase, the alteration of the metabolism is persistent but the modifications of the neurochemical profile in the IC are minor, consistent with a recovery phase with intervening partial tissue repair and defence mechanisms. For this second time point, MRS VOI was placed exactly at the same place as specified above, corresponding to the known site of the lesion on this model reported by Sizonenko et al. (4,11). Note that the VOI was out of the T_2W hypersignal remaining on several pups.

At the last time point, significant decrease of tNAA, Glu + Gln, and tCr was observed in the cortical lesion. The low tNAA provides evidence of persistent neuronal damage 22 days following HI. Indeed, the decreased Glu + Gln known as an excitatory neurotransmitter is due to the persistent altered neurotransmission and astrogliotic reaction. At this last time point, the neurochemical changes are related to the ongoing glial scar and neuronal damage because of the HI insult (5). The near complete recovery of the metabolic profile 22 days after injury, despite early metabolic changes and altered persistent macrostructure, is not unexpected. The injury happens on a developing brain with important ability to recover and adapt to damage by mechanisms that are often referred to as "developmental plasticity" (34,35). The consequences of the HI insult are different in newborns and adults, with a mix between reduced vulnerability compared with adults, increased defense mechanisms, and subsequent cerebral development. Further, a partial functional recovery of whisker elicited somatosensory cortex response is also present at P21 in this model despite altered cortex (36).

^{1}H MRS and MRI Relations

At all time points, no differences in the metabolic changes were detected between males and females. This indicates that the level of initial compromise is similar in both genders but results in different size of injury and CL between genders. This clearly supports differential vulnerability and repair between males and females that cannot only be attributed to gender differences in cell death pathways. At this point, we must emphasize that the neurochemical profile obtained with ^{1}H MRS measures only 17 metabolites in the brain in vivo and therefore limited cerebral metabolism mechanisms are evaluated. Thus, the absence of difference in the metabolic profile between males and females, despite anatomical differences, does not rule out differences in other nondetectable metabolic pathways leading to differential level of damage.

To find specific markers of the outcome following neonatal HI, correlations were assessed between percentage of variation of metabolite concentration at P4 and %CL at P25. As a result, the degree of CL at P25 was correlated with the variation of the concentration of Lac confirming that the degree of acute metabolic changes permits the early detection of the severity of the subsequent damage. The increase of Lac at P4 relates to the degree of injury at P25 confirming its clinical role as an early ischemia marker in HI injury (30,37). Several animal studies (38,39) have concluded that the secondary failure in cerebral energy status after HI is a significant contributor to the ultimate brain damage and neurologic compromise. This hypothesis is confirmed by our result where the variation of lactate concentration that can be used as a marker of secondary energy failure depth is linked to the long-term consequences following HI.

Longitudinally, the majority of the observed developmental changes of the neurochemical profile of the rat brain cortex (Fig. 3, Table 1) specifically the increase of NAA, Glu, Gln, and total Cr, the decrease of total Cho, PE, and Tau as well as the minor developmental changes in concentrations observed for GABA and NAAG are in excellent agreement with previously published data (16).

CONCLUSIONS

This is the first in vivo longitudinal assessment of anatomical and metabolic changes after HI at P3 in the developing brain using high-field MRI and localized ^{1}H MRS. We believe that the multimodal approach using MRI and MRS definitely offers new in vivo insight into the evolution of HI injury and subsequent alterations in brain development through neurochemical and anatomical assessment. We showed acute modifications within the IC of major metabolic components early after HI. These changes resulted from neuronal, glial, and metabolic reaction and compromise arising from the injury. In the long-term, defence/repair mechanisms together with cerebral development led to minor metabolic changes at P25 despite abnormal brain development with CL. Males and females showed different acute and long-term responses to the same initial injury. In addition to gender-different cell death mechanisms, differential vulnerability, repair and plasticity are possibly participating in the evolution of the damage. The potential of these early markers to predict long-term anatomical damage certainly needs further investigation prior to use in clinical practice. It could also be postulated that these markers will offer means of assessing the effects of therapeutic interventions in developing brain injury.

ACKNOWLEDGMENT

The authors thank Dr. Vladimir Mlynarik for his help in revising this manuscript.

REFERENCES

1. Larroque B, Ancel PY, Marret S, Marchand L, Andre M, Arnaud C, Pierrat V, Roze JC, Messer J, Thiriez G, Burguet A, Picaud JC, Breart G, Kaminski M. Neurodevelopmental disabilities and special care of

5-year-old children born before 33 weeks of gestation (the EPIPAGE study): a longitudinal cohort study. Lancet 2008;371:813–820.
2. Volpe JJ. Brain injury in premature infants: a complex amalgam of destructive and developmental disturbances. Lancet Neurol 2009;8: 110–124.
3. Hagberg H, Ichord R, Palmer C, Yager JY, Vannucci SJ. Animal models of developmental brain injury: relevance to human disease. A summary of the panel discussion from the Third Hershey Conference on Developmental Cerebral Blood Flow and Metabolism. Dev Neurosci 2002;24:364–366.
4. Sizonenko SV, Kiss JZ, Inder T, Gluckman PD, Williams CE. Distinctive neuropathologic alterations in the deep layers of the parietal cortex after moderate ischemic hypoxic injury in the P3 immature rat brain. Pediatr Res 2005;57:865–872.
5. Sizonenko SV, Sirimanne E, Mayall Y, Gluckman PD, Inder T, Williams C. Selective cortical alteration after hypoxic ischemic injury in the very immature rat brain. Pediatr Res 2003;54:263–269.
6. Nijboer CH, Kavelaars A, van Bel F, Heijnen CJ, Groenendaal F. Gender-dependent pathways of hypoxia–ischemia-induced cell death and neuroprotection in the immature P3 rat. Dev Neurosci 2007;29:385–392.
7. Renolleau S, Fau S, Charriaut-Marlangue C. Gender-related differences in apoptotic pathways after neonatal cerebral ischemia. Neuroscientist 2008;14:46–52.
8. Zhu C, Xu F, Wang X, Shibata M, Uchiyama Y, Blomgren K, Hagberg H. Different apoptotic mechanisms are activated in male and female brains after neonatal hypoxia–ischaemia. J Neurochem 2006;96: 1016–1027.
9. Bockhorst KH, Narayana PA, Liu R, Ahobila-Vijjula P, Ramu J, Kamel M, Wosik J, Bockhorst T, Hahn K, Hasan KM, Perez-Polo JR. Early postnatal development of rat brain: in vivo diffusion tensor imaging. J Neurosci Res 2008;86:1520–1528.
10. Fau S, Po C, Gillet B, Sizonenko S, Mariani J, Meric P, Charriaut-Marlangue C. Effect of the reperfusion after cerebral ischemia in neonatal rats using MRI monitoring. Exp Neurol 2007;208:297–304.
11. Sizonenko SV, Camm EJ, Garbow JR, Maier SE, Inder TE, Williams CE, Neil JJ, Huppi PS. Developmental changes and injury induced disruption of the radial organization of the cortex in the immature rat brain revealed by in vivo diffusion tensor MRI. Cereb Cortex 2007;17:2609–2617.
12. Wang S, Wu EX, Tam CN, Lau HF, Cheung PT, Khong PL. Characterization of white matter injury in a hypoxic ischemic neonatal rat model by diffusion tensor MRI. Stroke 2008;39:2348–2353.
13. Yang J, Wu EX. Detection of cortical gray matter lesion in the late phase of mild hypoxic ischemic injury by manganese-enhanced MRI. NeuroImage 2008;39:669–679.
14. Dubois J, Benders M, Borradori-Tolsa C, Cachia A, Lazeyras F, Ha-Vinh Leuchter R, Sizonenko SV, Warfield SK, Mangin JF, Huppi PS. Primary cortical folding in the human newborn: an early marker of later functional development. Brain 2008;131 (pt 8):2028–2041.
15. Inder TE, Warfield SK, Wang H, Huppi PS, Volpe JJ. Abnormal cerebral structure is present at term in premature infants. Pediatrics 2005;115:286–294.
16. Tkac I, Rao R, Georgieff MK, Gruetter R. Developmental and regional changes in the neurochemical profile of the rat brain determined by in vivo 1H NMR spectroscopy. Magn Reson Med 2003;50:24–32.
17. Lei H, Berthet C, Hirt L, Gruetter R. Evolution of the neurochemical profile after transient focal cerebral ischemia in the mouse brain. J Cereb Blood Flow Metab 2009;29:811–819.
18. Stadlin A, James A, Fiscus R, Wong YF, Rogers M, Haines C. Development of a postnatal 3-day-old rat model of mild hypoxic ischemic brain injury. Brain Res 2003;993:101–110.
19. Gruetter R, Tkac I. Field mapping without reference scan using asymmetric echo-planar techniques. Magn Reson Med 2000;43: 319–323.
20. Mlynarik V, Gambarota G, Frenkel H, Gruetter R. Localized short-echo-time proton MR spectroscopy with full signal-intensity acquisition. Magn Reson Med 2006;56:965–970.
21. Provencher SW. Estimation of metabolite concentrations from localized in vivo proton NMR spectra. Magn Reson Med 1993;30:672–679.
22. Pfeuffer J, Tkac I, Provencher SW, Gruetter R. Toward an in vivo neurochemical profile: quantification of 18 metabolites in short-echo-time (1)H NMR spectra of the rat brain. J Magn Reson 1999;141:104–120.
23. Rivière D, Régis J, Cointepas Y, Papadopoulos-Orfanos D, Cachia A, Mangin J-F. A freely available Anatomist/BrainVISA package for structural morphometry of the cortical sulci. In Proceedings of the. 9th annual meeting of HBM, New York, USA, 2003. Neuroimage 19(2), p. 934.
24. Loubinoux I, Volk A, Borredon J, Guirimand S, Tiffon B, Seylaz J, Meric P. Spreading of vasogenic edema and cytotoxic edema assessed by quantitative diffusion and T_2 magnetic resonance imaging. Stroke 1997;28:419–426; discussion 426–417.
25. Verheul HB, Berkelbach van der Sprenkel JW, Tulleken CA, Tamminga KS, Nicolay K. Temporal evolution of focal cerebral ischemia in the rat assessed by T_2-weighted and diffusion-weighted magnetic resonance imaging. Brain Topogr 1992;5:171–176.
26. Welch KM, Cao Y, Nagesh V. Magnetic resonance assessment of acute and chronic stroke. Prog Cardiovasc Dis 2000;43:113–134.
27. Marchetti B, Gallo F, Farinella Z, Tirolo C, Testa N, Caniglia S, Morale MC. Gender, neuroendocrine-immune interactions and neuron-glial plasticity. Role of luteinizing hormone-releasing hormone (LHRH). Ann N Y Acad Sci 2000;917:678–709.
28. Lanfermann H, Kugel H, Heindel W, Herholz K, Heiss WD, Lackner K. Metabolic changes in acute and subacute cerebral infarctions: findings at proton MR spectroscopic imaging. Radiology 1995;196:203–210.
29. Schurr A, Payne RS, Miller JJ, Rigor BM. Brain lactate is an obligatory aerobic energy substrate for functional recovery after hypoxia: further in vitro validation. J Neurochem 1997;69:423–426.
30. Penrice J, Lorek A, Cady EB, Amess PN, Wylezinska M, Cooper CE, D'Souza P, Brown GC, Kirkbride V, Edwards AD, Wyatt JS, Reynolds EO. Proton magnetic resonance spectroscopy of the brain during acute hypoxia–ischemia and delayed cerebral energy failure in the newborn piglet. Pediatr Res 1997;41:795–802.
31. Vannucci RC, Towfighi J, Vannucci SJ. Secondary energy failure after cerebral hypoxia–ischemia in the immature rat. J Cereb Blood Flow Metab 2004;24:1090–1097.
32. Gruetter R, Seaquist ER, Kim S, Ugurbil K. Localized in vivo 13C-NMR of glutamate metabolism in the human brain: initial results at 4 tesla. Dev Neurosci 1998;20:380–388.
33. Tkac I, Keene CD, Pfeuffer J, Low WC, Gruetter R. Metabolic changes in quinolinic acid-lesioned rat striatum detected non-invasively by in vivo (1)H NMR spectroscopy. J Neurosci Res 2001;66:891–898.
34. Sizonenko SV, Bednarek N, Gressens P. Growth factors and plasticity. Semin Fetal Neonatal Med 2007;12:241–249.
35. Casey BJ. Brain plasticity, learning, and developmental disabilities. Ment Retard Dev Disabil Res Rev 2003;9:133–134.
36. Quairiaux C, Sizonenko SV, Megevand P, Michel CM, Kiss JZ. Functional deficit and recovery of developing sensorimotor networks following neonatal hypoxic ischemic injury in the rat. Cereb Cortex 2010;20:2080–2091.
37. Malisza KL, Kozlowski P, Peeling J. A review of in vivo 1H magnetic resonance spectroscopy of cerebral ischemia in rats. Biochem Cell Biol 1998;76:487–496.
38. Taylor DL, Edwards AD, Mehmet H. Oxidative metabolism, apoptosis and perinatal brain injury. Brain Pathol 1999;9:93–117.
39. Williams CE, Gunn AJ, Mallard C, Gluckman PD. Outcome after ischemia in the developing sheep brain: an electroencephalographic and histological study. Ann Neurol 1992;31:14–21.